Am J Physiol Renal Physiol 289: F891–F901, 2005.
First published May 24, 2005; doi:10.1152/ajprenal.00019.2005.

Vascular ENaC proteins are required for renal myogenic constriction

Nikki L. Jernigan and Heather A. Drummond

Department of Physiology and Biophysics and the Center for Excellence in Cardiovascular Renal Research, University of Mississippi Medical Center, Jackson, Mississippi

Submitted 19 January 2005; accepted in final form 20 May 2005

Jernigan, Nikki L., and Heather A. Drummond. Vascular ENaC proteins are required for renal myogenic constriction. *Am J Physiol Renal Physiol* 289: F891–F901, 2005. First published May 24, 2005; doi:10.1152/ajprenal.00019.2005.—The myogenic response is an essential component of renal blood flow autoregulation and is the inherent ability of vascular smooth muscle cells (VSMCs) to contract in response to increases in intraluminal pressure. Although mechanosensitive ion channels are thought to initiate VSMC stretch-induced contraction, their molecular identity is unknown. Recent reports suggest degenerin/epithelial Na^+ channels (DEG/ENaC) may form mechanotransducers in sensory neurons and VSMCs; however, the role of DEG/ENaC proteins in myogenic constriction of mouse renal arteries has not been established. To test the hypothesis that DEG/ENaC proteins are required for myogenic constriction in renal vessels, we first determined expression of ENaC transcripts and proteins in mouse renal VSMCs. Then, we determined pressure- and agonist-induced constriction and changes in vascular smooth muscle cytosolic Ca^{2+} and Na^+ in isolated mouse renal interlobar arteries following DEG/ENaC inhibition with amiloride and benzamil. We detect α-, β-, and γENaC transcript and protein expression in cultured mouse renal VSMC. In contrast, we detect only β- and γ- but not αENaC protein in freshly dispersed mrVMSC. Selective DEG/ENaC inhibition, with low doses of amiloride and benzamil, abolishes pressure-induced constriction and increases in cytosolic Ca^{2+} and Na^+ without diminishing agonist-induced responses in isolated mouse interlobar arteries. Our findings indicate that DEG/ENaC proteins are required for myogenic constriction in mouse interlobar arteries and are consistent with our hypothesis that DEG/ENaC proteins may be components of mechanosensitive ion channel complexes required for myogenic vasoconstriction.

mechanotransduction; renal blood flow autoregulation; amiloride; benzamil; isolated renal vessel; stretch-activated cation channel; calcium; sodium

MYOGENIC VASOCONSTRICTION is an intrinsic property of most resistance vessels characterized by a decrease in luminal diameter in response to an increase in intraluminal pressure. The response is important in establishing basal vascular tone and maintaining blood flow autoregulation. It is well established that vascular smooth muscle (VSM) membrane depolarization and subsequent Ca^{2+} influx via voltage-gated Ca^{2+} channels mediate myogenic constriction (23, 32, 36). However, the mechanism that transduces mechanical stimuli (pressure-induced stretch) into a cellular event (depolarization) is less understood. Although mechanosensitive nonselective cation channels are thought to initiate pressure-induced depolarization (9, 29, 38, 46), the molecule(s) involved has not been identified.

Members of the degenerin/epithelial Na^+ channel (DEG/ENaC) family have recently been identified as mechanosensors in a variety of species and cell types (2, 17, 20, 28, 33). In mammals, DEG/ENaC proteins are found at several important sites of mechanotransduction, including dorsal root ganglion, arterial baroreflex sensory neurons, osteoblasts, keratinocytes, and vascular smooth muscle cells (VSMCs) (5, 12–14, 18, 30, 34). Two subfamilies of proteins are expressed in mammals: ENaC and acid-sensing ion channel. Acid-sensing ion channel proteins are activated by protons and have only been identified in neural tissue and sensory epithelia (33, 45). ENaC proteins are expressed in a diverse range of cell types but are highly expressed in epithelial cells of the kidney, lung, and colon, where they play a rate-limiting role in Na^+ and water transport (2, 6, 17, 20, 28, 33). Because DEG/ENaC family members are required for mechanotransduction in many species and share similar single-channel conductance with mammalian mechanosensitive ion channels found in VSMCs (10, 26), ENaC proteins may also be required for mechanotransduction in VSMCs.

Recently, our laboratory demonstrated the presence of β- and γENaC transcripts and proteins in rat cerebral VSM. Furthermore, the specific ENaC inhibitors, amiloride and benzamil, were found to block pressure-induced constriction in isolated rat middle cerebral arteries (14). These data provide evidence that DEG/ENaC proteins may be involved in the myogenic response. Similar to cerebral blood flow, renal blood flow is tightly autoregulated, a presumed protective mechanism against target end-organ injury due to hypertension. Therefore, we hypothesize ENaC proteins are expressed in mouse renal VSM and are required for myogenic vasoconstriction. To test this hypothesis, we first determined whether α-, β-, and γENaC transcripts and proteins are expressed in mouse renal VSMCs (mrVSMCs) using RT-PCR, immunoblotting, and immunolocalization. We then examined the effect of the specific DEG/ENaC inhibitors, amiloride and benzamil, on myogenic- and agonist-induced vasoreactivity and changes in cytosolic Ca^{2+} and Na^+ in isolated mouse interlobar arteries. Our findings suggest that ENaC proteins are expressed in mrVSMCs and play a pivotal role in the myogenic response.

METHODS

All protocols and procedures employed in this study were reviewed and approved by the Institutional Animal Care and Use Committee of the University of Mississippi Medical Center.

Antibody Description and Characterization

A rabbit anti-α-ENaC antibody was obtained from Chemicon and used for immunolocalization (1:200) and Western blotting (1:1,000). A rabbit anti-β-ENaC antibody, directed to the COOH terminus

Address for reprint requests and other correspondence: H. A. Drummond, Dept. of Physiology and Biophysics, Univ. of Mississippi Medical Center, 2500 North State St., Jackson, MS 39216 (e-mail: hdrummond@physiology.umsmed.edu).

The costs of publication of this article were defrayed in part by the payment of page charges. The article must therefore be hereby marked "*advertisement*" in accordance with 18 U.S.C. Section 1734 solely to indicate this fact.

(1:100), and a sheep anti-β-ENaC antibody, directed to the NH_2 terminus (1:2,500), were used for immunostaining and Western blotting, respectively (12, 14). A sheep anti-γ-ENaC antibody was used for immunostaining (1:100) and Western blotting (1:2,500) (14). To determine specificity of the anti-ENaC antibodies, we used immunolabeling and Western blot analysis in transiently transfected COS-7 cells and Western blot in mouse lung tissue.

COS-7 cells were plated on eight-well glass slides or 100-mm dishes for immunostaining and Western blot analysis, respectively. Cells were transiently transfected with the ENaC cDNA constructs using Lipofectamine 2000 (Invitrogen, Carlsbad, CA) according to the manufacturer's instructions and grown for 48 h before harvesting. To evaluate the rabbit anti-αENaC antibody, we used αrENaC (where r designates rat) (12). To evaluate the rabbit anti-βENaC antibody for immunolabeling, we used an enhanced green fluorescence protein (EGFP) fusion construct encoding for full-length βmENaC (where m designates mouse; EGFP-βENaC). To evaluate the sheep anti-βENaC antibody for Western blot analysis, we used an EGFP fusion construct encoding for the NH_2-terminal region of βrENaC (EGFP-$\beta ENaC_{I41X}$). To evaluate the sheep anti-γENaC antibody, we used an EGFP fusion construct encoding for the NH_2-terminal region of γrENaC (EGFP-$\gamma ENaC_{L160x}$). We used EGFP fusion constructs when possible as an independent method to identify transfected cells. All constructs were generated using standard PCR cloning techniques and sequenced to confirm identity.

For immunolabeling, cells were rinsed in PBS and fixed in 4% paraformaldehyde for 10 min before immunolabeling. Samples were blocked with 5% normal donkey serum for 1 h and then incubated with the primary antibodies for 1 h (αENaC, 1:200; βENaC, 1:100; γENaC, 1:100). After rinsing with PBS, the samples were incubated with Cy3-conjugated donkey anti-rabbit IgG (1:100, Jackson Immunological, West Grove, PA) or Alexa 546-conjugated donkey anti-sheep IgG (1:1,000; Molecular Probes, Eugene, OR). As controls, samples were treated as above except the primary antibody was incubated overnight at 4°C with the antigenic molecule (~10 μg/ml). Samples were examined using fluorescence confocal microscopy (TCS-SP2, Leica Microsystems), and images were prepared in Photoshop and Illustrator (Adobe). Specificity of the anti-ENaC antibodies using immunolabeling is shown in Fig. 1, *A–C*. αENaC immunolabeling (Fig. 1*A*) is blocked by coincubation with the αENaC antigen. The β- and γENaC immunostaining is present only the EGFP-labeled cells and blocked by coincubation with the appropriate antigen (Fig. 1, *B* and *C*).

We used standard Western blotting approaches to determine the specificity of the anti-ENaC antibodies. Lysates were obtained by scraping transiently transfected COS-7 cells or homogenizing mouse lung tissue (see below) in lysis solution [50 mM Tris·HCl-150 mM NaCl, 1% Triton X-100, 1× protease cocktail inhibitor (Pierce, Rockford, IL), 1× EDTA (Pierce), and 1% sodium deoxycholate]. Samples were sonicated briefly, vortexed, incubated for 20 min and centrifuged at 14,000 *g* for 20 min. From preliminary experiments, the strongest signals were detected in the Triton X-100-insoluble fraction for COS-7 cells and the soluble fraction for lung tissue. Protein samples (~50 μg) were separated on SDS-PAGE gels (7.5, 10, and 12.5%; Bio-Rad, Hercules, CA) using the Criterion System (Bio-Rad). Precision Plus protein standards (Bio-Rad) were used to estimate molecular weight. After electrophoresis, the products were transferred to nitrocellulose at 40 V for 2 h. Membranes were rinsed with PBS and blocked with Odyssey blocking buffer (Li-Cor Biosystems, Lincoln, NE) for 1 h and incubated with the primary antibodies for 3 h. Samples were rinsed in PBS plus 0.1% Tween 20 and then incubated with IR700 dye-conjugated donkey anti-rabbit or anti-sheep IgG for 1 h and rinsed thoroughly. As controls, samples were treated as above except the primary antibody was incubated overnight with the antigen (10 μg/ml). Membrane staining (antibody and antibody + antigen) was visualized simultaneously with an Odyssey infrared scanner (Li-Cor). Images were prepared for presentation in Photoshop and Illustrator (Adobe). As shown in Fig. 1, the anti-ENaC antibodies detected products near the predicted size for αENaC (near 75–80 kDa; Fig. 1*D*), EGFP-$\beta ENaC_{I41X}$ (34 kDa; Fig. 1*E*), and EGFP-$\gamma ENaC_{L160X}$ (45 kDa; Fig. 1*F*) and were blocked by coincubation with the antigen.

Anti-ENaC antibody specificity was also evaluated in mouse lung samples. The rabbit anti-αENaC antibody detected a product below the predicted size (near 75 kDa; Fig. 1*G*) that was blocked by the presence of the antigen. The sheep anti-β- and anti-γENaC antibodies also detected bands near the predicted sizes (70–75 kDa; Figs. 1, *H* and *I*) that were blocked by antigen incubation. Therefore, in both heterologous cells and native tissue, the anti-ENaC antibodies detect products near the expected size, which is blocked by coincubation with the antigens.

Freshly Dispersed mrVSMCs

To disperse mrVSMCs, we used a modification of a previously published protocol (47). Briefly, dissected renal vessels from male C57BL/6J mice (6–8 wk; Jackson Laboratory, Bar Harbor, ME) were enzymatically digested in HBSS containing 26 U/ml papain and 1 mg/ml ditheoerythritol for 15 min at 37°C, followed by HBSS plus 2 U/ml collagenase, 1 mg/ml soybean trypsin inhibitor, and 75 U/ml elastase for 12 min at 37°C. The vessels were rinsed with HBSS and gently triturated with a fire-polished plugged Pasteur pipette to dissociate cells. Samples were filtered over a 70-μm filter and examined microscopically for dispersion.

ENaC Immunolocalization in Freshly Dispersed mrVSMCs.

To determine ENaC protein expression and localization, freshly dispersed mrVSMCs were fixed in 4% paraformaldehyde while in suspension and then air-dried to glass slides overnight at 37°C. After rehydrating and washing in PBS, samples were permeabilized with 0.1% Triton X-100 and blocked with 5% normal donkey serum or tyramide blocking solution in PBS for 1 h before addition of primary antibodies. Samples were incubated overnight at 4°C with mouse anti-α-actin (1:200; Sigma), rabbit anti-αENaC (1:100; Chemicon), rabbit anti-βENaC (1:100), or/and sheep anti-γENaC (1:50). Samples were washed with PBS and incubated with secondary antibodies for 1 h. To determine the specificity of the primary antibodies, parallel samples were prepared as above except the primary antibodies were preincubated with the appropriate antigens (10 μg/ml). To enhance immunostaining, we used the tyramide amplification system (Molecular Probes) with the rabbit anti-αENaC and sheep anti-γENaC antibodies. We examined all samples using fluorescence confocal microscopy. Experimental and control (antigen) samples were examined in parallel under identical conditions. Images were captured sequentially to eliminate bleed-through artifacts and prepared using Photoshop 6.0 and Illustrator 10 (Adobe Systems).

mrVSMCs Isolation and Culture

We wanted to determine whether ENaC transcripts are expressed in VSMCs; however, potential epithelial cell contamination in our dissociated VSMC preparation presented a risk for RT-PCR analysis. Therefore, to avoid this, we isolated the VSMCs, using a modified version of a previously published protocol (15), and grew the cells in culture in the presence of amphotericin B, a potent nephrotoxic agent, to prevent epithelial cell contamination. At each passage, samples were immunoassayed for α-actin expression, a smooth muscle cell marker. Briefly, male C57BL/6J mice (6–8 wk; Jackson Laboratory) were anesthetized with pentobarbital sodium. PBS was flushed through the renal vasculature to clear the blood before perfusing with a 5% suspension of iron oxide particles in *media 1* [DMEM (GIBCO) containing 100 U/ml penicillin, 100 μg/ml streptomycin, 100 U/ml amphotericin B, and 25 mM HEPES]. The kidneys were rapidly excised and placed in *media 1*, where they were minced and dispersed by passing through a sterile wire screen (stainless steel, 30 mesh) and

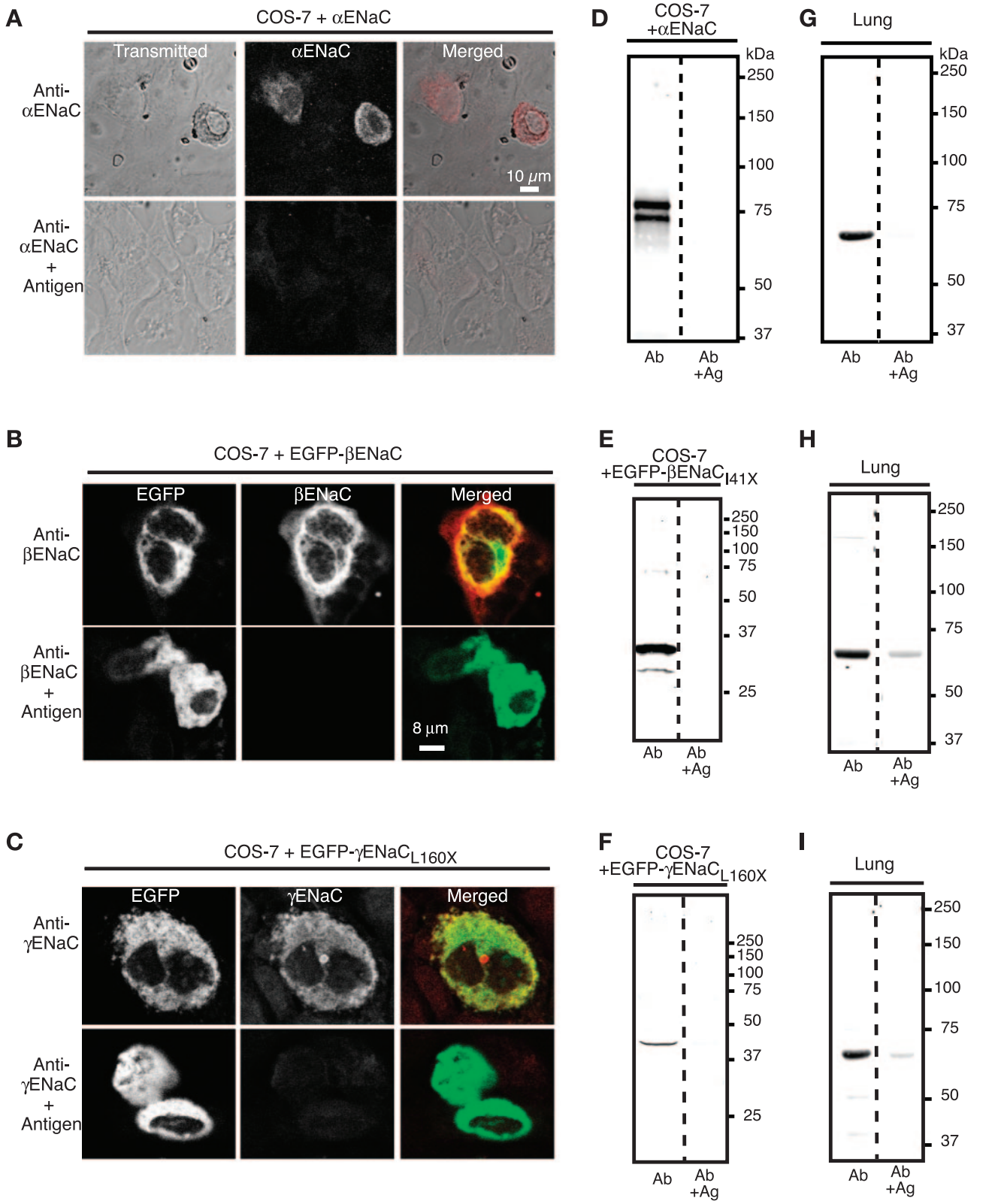

Fig. 1. The anti α-, β-, and γENaC antibodies specifically detect epithelial Na^+ channel (ENaC) proteins by immunolabeling and Western blotting. The anti α-, β-, and γENaC antibodies detect respective ENaC molecules in COS-7 cells expressing αENaC (*A*), EGFP-βENaC (*B*), and EGFP-$\gamma ENaC_{L160x}$ (*C*). Incubation with the corresponding antigen (+Ag) blocks immunolabeling. Using Western blotting, the anti α-, β-, and γENaC antibodies detect bands near the expected size for αENaC (*D*; 75–80 kDa), $EGFP_{\beta I41X}$ (*E*; 34 kDa), and $EGFP\gamma_{L160X}$ (*F*; 45 kDa) in transiently transfected COS-7 cells, which are blocked by antigen incubation. In mouse lung tissue, the anti-ENaC antibodies detect bands near the predicted sizes for αENaC (*G*; 75 kDa), βENaC (*H*; 70–75 kDa), and γENaC (*I*; 70–75 kDa) and were blocked by antigen competition.

Table 1. *RT-PCR oligonucleotide sequences*

Target	Forward Primer Sequence (5′-3′)	Reverse Primer Sequence (5′-3′)	Annealing Temperature, °C	Product Size, bp
αENaC	TAAACTGCAGGCTGCCTTCT	ATGTAGGGTGGGGACAGAAA	55	474
nested	GATAGCCTGGGCTGCTTCTCC	GGTAGAGGCCACCTCCCT	55	425
βENaC	AAAGGCCTGCGCAGGAGGCGGCCACAG	GATGGCCTCCACCTCACTGTCCGACTC	60	225
γENaC	GAGATGCTCCTGTCTAACTTT	GTCCAAGCGCAAGGTATTGTA	55	326

Forward and reverse primer sequences, annealing temperature, and predicted product size for PCR amplification of epithelial Na^+ channel (ENaC) transcripts in cultured mouse renal vascular smooth muscle cells are indicated.

collected into 50-ml conical tubes. A magnet was placed against the collection tube to secure the iron-laden microvessels in the tube while the remaining tissue was decanted. The microvessels were placed in *media 1* containing 0.6 mg/ml of collagenase type IV (Sigma) and incubated in a shaking incubator at 37°C for 15 min. The vessels were resuspended in *media 2* (same as *media 1* plus 13 mM $NaHCO_3$, and 20% FBS) and plated in culture flasks. The VSMCs were incubated in 5% CO_2-95% air at 37°C and 98% humidity, and the media were changed every 48 h until confluency. These cells were used between *passages 3* and *6* for RT-PCR, immunolocalization, and Western blot analysis.

ENaC Transcript Expression in Cultured mrVMSCs

We used RT-PCR to determine whether α-, β-, and γENaC transcripts are expressed in cultured mrVSMCs. Total RNA was isolated using RNA Stat-60 (Tel-Test "B"); DNase was treated and reverse transcribed with a reverse transcription system (Promega, Madison, WI). The PCR primer sequences and conditions are listed in Table 1. PCR products were separated using gel electrophoresis, visualized with ethidium bromide, and sequenced to confirm identity.

ENaC Immunolocalization in Cultured mrVSMCs

Similar methods were used to determine ENaC immunolocalization in cultured mrVSMCs as for the freshly dispersed mrVSMCs.

Western Blot Detection of ENaC Proteins in Cultured mrVSMCs

To determine whether α-, β-, and γENaC protein were expressed in renal VSM, cultured mrVSMCs were homogenized in lysis buffer

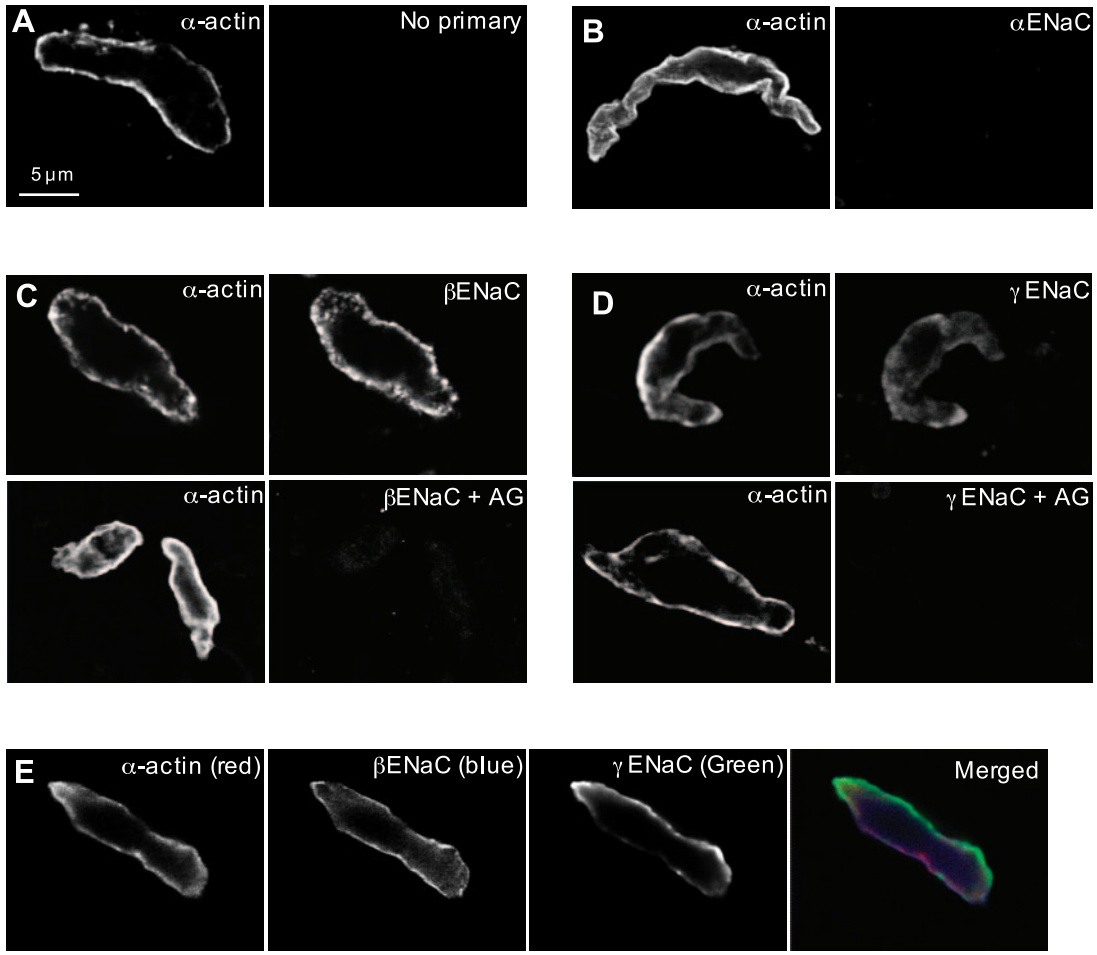

Fig. 2. Immunolabeling of α-actin and α-, β-, and γENaC, protein expression in freshly dispersed mouse renal vascular smooth muscle cells (mrVMSC). α-Actin, used as a positive control to identify smooth muscle cells, is shown at *left* in *A–E*. A no-primary antibody control is shown in *A*, *right*. αENaC protein was not detected in α-actin-labeled freshly dispersed mrVSMCs (*B*, *right*). βENaC (*C*, *right*) and γENaC (*D*, *right*) proteins were detected in α-actin labeled mrVSMCs. β- and γENaC colocalize in α-actin-labeled mrVSMCs (*E*). βENaC and γENaC immunolabeling was blocked by antigen competition (+Ag).

containing (in mM) 50 Tris·HCl, 150 NaCl, 1% Triton X-100, 2× Halt Protease Inhibitor Cocktail, and 1× EDTA. After homogenization, samples were vortexed, sonicated, and incubated on ice for 5 min. Samples were centrifuged at 16,000 *g* for 15 min at 4°C to remove insoluble debris. The supernatant was collected, and protein content was determined by Bio-Rad DC protein assay. Proteins (25 μg) were separated on SDS-PAGE gel and transferred to a PVDF membrane. Membranes were rinsed briefly in PBS and blocked with Odyssey blocking buffer (Li-Cor Biosciences) for 1 h at room temperature. Blots were probed with rabbit anti-αENaC (1:500, Chemicon), sheep anti-βENaC (1:1,000), and sheep anti-γENaC (1:1,000). All blots were rinsed in PBS plus 0.05% Tween 20 and incubated with Alexa 680-conjugated donkey anti-sheep IgG (1:2,000; Molecular Probes) or IRDye 800-conjugated donkey anti-rabbit IgG (1:2,000; Rockland) for 1 h at room temperature. After they were rinsed in PBS plus 0.05% Tween 20 and had a final rinse in PBS, membranes were examined using the Odyssey infrared imaging system. Images were prepared in Photoshop and Illustrator.

Cannulation of Mouse Interlobar Arteries for Dimensional and Cytosolic Ca^{2+}/Na^{+} Analysis

Male C57BL/6J mice (6–8 wk; Jackson Laboratory) were anesthetized with halothane and decapitated. Kidneys were excised and placed in ice-cold physiological saline solution [PSS; pH adjusted to 7.4 with NaOH, containing (in mM) 130 NaCl, 4 KCl, 1.2 $MgSO_4$, 4 $NaHCO_3$, 1.8 $CaCl_2$, 10 HEPES, 1.18 KH_2PO_4, 6 glucose, and 0.03 EDTA]. Kidneys were hemisected, and interlobar arteries (0.5–1 mm length; without side branches; 78 ± 23 μm active inner diameter at 75 mmHg, vehicle treated) were dissected from surrounding kidney tissue. Vessels were transferred to a vessel chamber (Living Systems model CH/1/SH, Burlington, VT), and the proximal end of the artery was cannulated with a tapered glass pipette, secured in place with a single strand of silk ligature, and gently flushed to remove any blood from the lumen. Next, the distal end of the vessel was cannulated, and the artery was gently stretched longitudinally to approximate its in situ length and pressurized to 75 mmHg and warmed to 37°C. All vessels were studied under stop flow conditions to eliminate potential effects of flow-induced shear stress. The vessel chamber was mounted on a Nikon Eclipse TE200 microscope equipped with a CoolSnap CCD camera (Roper Scientific, Trenton, NJ). Images were analyzed using MetaMorph software (Universal Imaging, Dowingtown, PA) to determine vessel inner diameter.

Experimental Protocols

Effect of ENaC inhibition on myogenic vasoreactivity. After an initial incubation period (30 min at 75 mmHg), a pressure-diameter curve was generated to determine the effect of ENaC inhibition on myogenic constriction. Arteries were exposed to step-wise increases in intraluminal pressure from 25 to 150 mmHg (25 mmHg steps, 5 min each). Intraluminal pressure was then reduced to 75 mmHg, and arteries were equilibrated for 30 min with Ca^{2+}-free PSS (in mM: 130 NaCl, 4 KCl, 1.2 $MgSO_4$, 4 $NaHCO_3$, 10 HEPES, 1.18 KH_2PO_4, 6

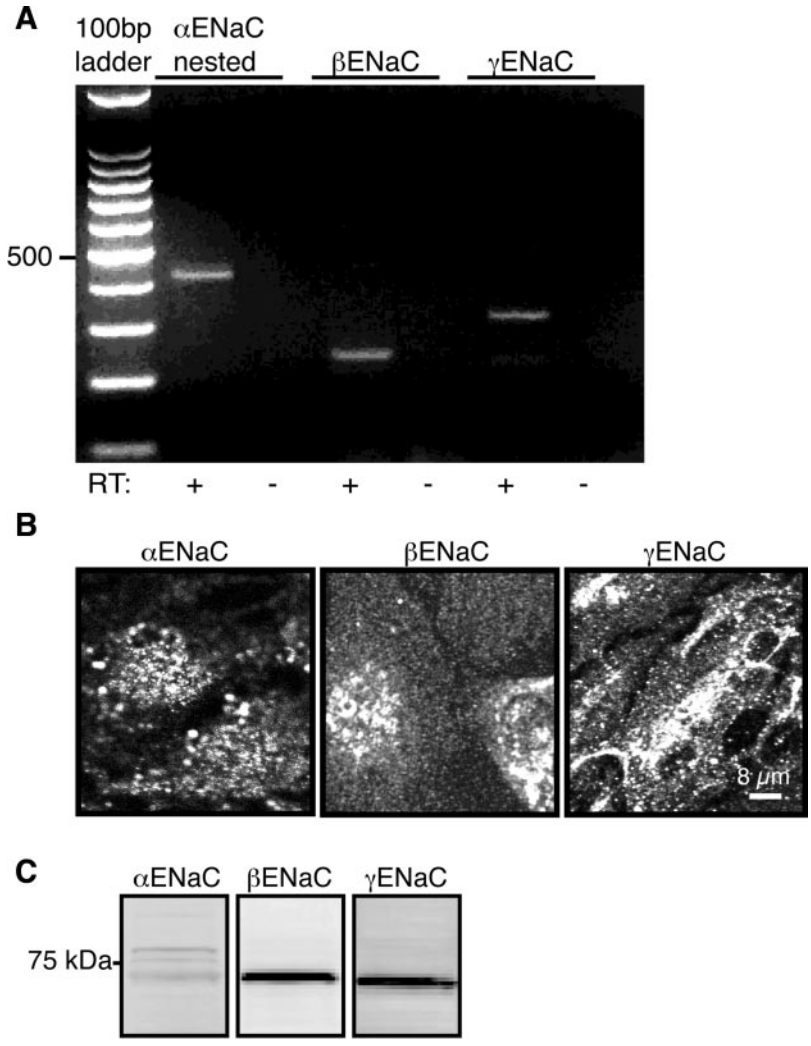

Fig. 3. Analysis of α-, β-, and γENaC transcript and protein expression in cultured mrVSMC. *A*: RT-PCR detection of α-, β-, and γENaC transcripts. The presence (+) and absence (−) of RT is indicated. Nested PCR was used to detect αENaC expression. *B*: punctuate cytoplasmic and/or perinuclear immunolocalization of α-, β-, and γENaC protein in cultured mrVSMCs. *C*: Western blot analysis of ENaC expression in cultured mrVSMCs. Products near the theoretical molecular mass of α-, β-, and γENaC proteins (70–80 kDa) were found.

glucose, 0.03 EDTA, and 2 EGTA) to determine the passive pressure-diameter curve as described above. This protocol was repeated in the presence of the specific ENaC inhibitors amiloride (1 and 5 μM) or benzamil (0.1 and 1 μM). The ENaC inhibitors were present in the bath and lumen of the vessel. Myogenic tone was calculated as the percent difference between the active (PSS) and passive (Ca^{2+}-free PSS) inner diameter at each pressure.

Effect of ENaC blockade on phenylephrine- and ACh-induced vasoreactivity. To determine whether amiloride (1 and 5 μM) or benzamil (0.1 and 1 μM) altered vasoconstrictor reactivity, we assessed vasoconstriction to the α_1-adrenergic receptor agonist, phenylephrine (PE; 10^{-9}–10^{-5} M) in the presence of amiloride (1 and 5 μM) and benzamil (0.1 and 1 μM). PE concentration response curves were performed in Ca^{2+}-free PSS to verify vascular tone was eliminated under Ca^{2+}-free condition. PE-induced vasoconstrictor responses were calculated as percent of baseline inner diameter. To determine nonspecific effects of amiloride and benzamil on endothelium-dependent vasodilation, we examined responses to the endothelium-dependent dilator ACh (1 μM) in arteries preconstricted with PE (10^{-5} M). ACh-mediated vasodilation was calculated as percent reversal of PE-induced vasoconstriction.

Effect of ENaC inhibition on pressure- and KCl-induced increases in cytosolic Ca^{2+} and Na^{+}. Fluorescence ion indicator dyes calcium orange-AM and sodium green-AM (Molecular Probes) were used to determine the effect of ENaC inhibition on pressure- and KCl-induced increases in cytosolic Ca^{2+} and Na^{+}. Mouse interlobar arteries were cannulated as described. Pressurized arteries (75 mmHg) were simultaneously loaded abluminally with calcium orange and sodium green (2 μM in PSS and 0.05% pluronic acid) and incubated for 30 min at 37°C in the dark. After dye loading, vessels were rinsed three times over 15 min with PSS (37°C) to wash out excess dye to allow for hydrolysis of AM groups by intracellular esterases. The indicator dyes were excited using a Lamba DG4 high-speed filter changer (Sutter Instruments, Novato, CA) and standard tetramethylrhodamine isothiocyanate and fluorescein isothiocyanate excitation/emission filter sets. Changes in Ca^{2+} fluorescence (F_{Ca}) and Na^{+} fluorescence (F_{Na}) intensity in response to an increase in intraluminal pressure from 50 to 125 mmHg (one step) and KCl (50 mM) were assessed from background-subtracted fluorescence images collected at 1 frame/s (over 5 min) using a high-speed, high-sensitivity Pentamax intensified CCD camera (Princeton Instruments, Roper Scientific, Trenton, NJ). Background fluorescence was collected before dye loading. Changes in F_{Ca} and F_{Na} intensities were calculated as the percent increase from baseline (for KCl) and 50 mmHg (for pressure). In a few vessels, we evaluated the effect of amiloride and benzamil on baseline F_{Ca} and F_{Na} by recording fluorescence intensity before and after administration of the inhibitors.

Statistics

All data are expressed as means ± SD. A one-way ANOVA or two-way ANOVA with repeated measures was used to make comparisons where appropriate. Differences among groups were compared using the Student-Newman-Keuls test. Statistical significance was considered at $P < 0.05$.

RESULTS

ENaC Immunolocalization in Freshly Dispersed mrVSMCs

In freshly dispersed mrVSMCs, we were unable to detect expression of αENaC protein, even after signal amplification using the tyramide amplification system (Molecular Probes) (Fig. 2*B*). Expression of β- and γENaC proteins was detected in α-actin-labeled dispersed VSMCs and was blocked by incubation with the corresponding antigens (Fig. 2, *C* and *D*). As shown in Fig. 2*E*, β- and γENaC are expressed within the same cell. Immunostaining for β- and γENaC was similar to α-actin, suggesting they are expressed at or near the cell membrane.

ENaC Expression in Cultured mrVSMC

Using RT-PCR, immunolocalization, and Western blotting, we detected expression of α-, β-, and γENaC transcripts and

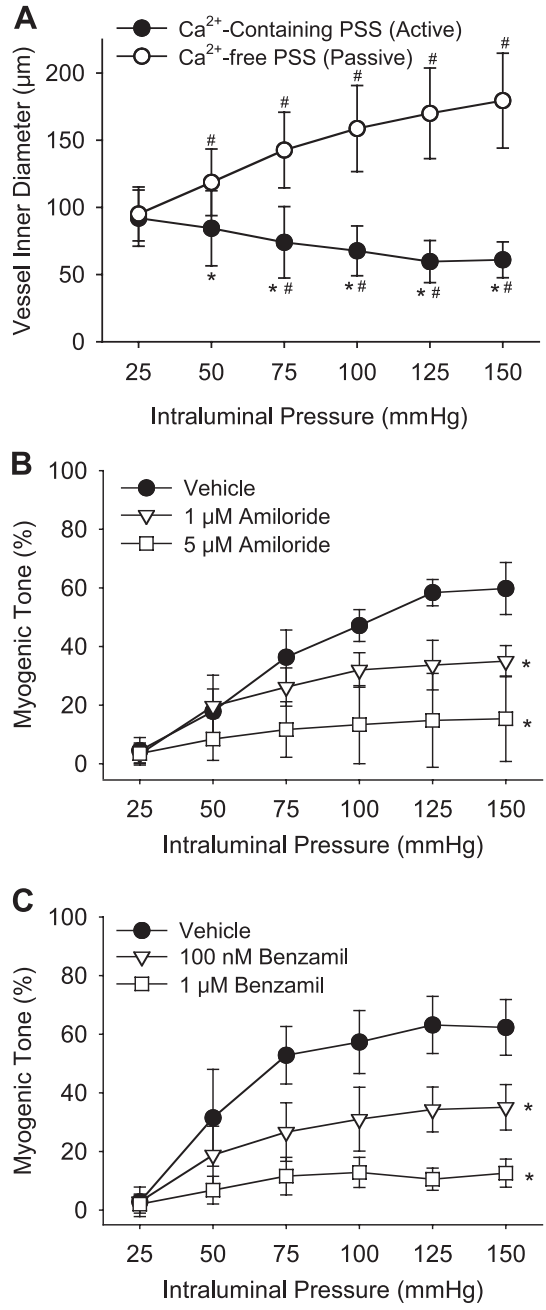

Fig. 4. ENaC inhibition blocks myogenic constriction in isolated mouse interlobar arteries. *A*: change in vessel inner diameter to increases in intraluminal pressure. Vessels constrict to increases in intraluminal pressure in Ca^{2+}-containing PSS (active tone; ●; $n = 9$) and dilate to increases in intraluminal pressure in Ca^{2+}-free PSS (passive tone; ○; $n = 9$). For *B* and *C*, %myogenic tone was calculated as the percent difference between the active and passive tone. *B*: amiloride, in a concentration-dependent manner (1 and 5 μM; $n = 6$), inhibits myogenic tone. *C*: benzamil (0.1 and 1 μM; $n = 6$), an amiloride analog, also blocks myogenic tone. Values are means ± SD. In *A*: #$P < 0.05$ vs. 25 mmHg and *$P < 0.05$ vs. Ca^{2+}-free PSS. In *B* and *C*: *$P < 0.05$ vs. vehicle.

Table 2. *Effect of amiloride and benzamil on active and passive vessel inner diameter and baseline calcium orange and sodium green fluorescence intensity*

	Amiloride Concentration, μM			Benzamil Concentration, μM		
	0	1	5	0	0.1	1
Inner diameter, μm	$n = 6$	$n = 6$	$n = 6$	$n = 6$	$n = 6$	$n = 6$
Active (75 mmHg)	88 (SD 27)	122 (SD 18)*	142 (SD 15)*	67 (SD 16)	100 (SD 35)*	117 (SD 12)*
Passive (75 mmHg)	149 (SD 33)	166 (SD 25)	152 (SD 25)	144 (SD 24)	136 (SD 44)	130 (SD 20)
Baseline fluorescence intensity, FIU	$n = 3$		$n = 3$	$n = 3$		$n = 3$
Calcium F_{615} (50 mmHg)	1,482 (SD 687)		1,457 (SD 634)	1,862 (SD 560)		1,853 (SD 626)
Sodium F_{532} (50 mmHg)	309 (SD 82)		318 (SD 91)	381 (SD 91)		357 (SD 67)

Values are means ± SD; n = no. of experiments. FIU, fluorescence intensity units. *$P < 0.05$ vs. corresponding vehicle.

proteins in cultured mrVSMCs (Fig. 3). ENaC immunostaining was punctate in nature and localized primarily within the cytoplasm; however, occasional perinuclear staining was also observed. With the use of Western blot analysis, anti-ENaC antibodies detected major bands near the predicted molecular weights of ENaC molecules (70–78 kDa) in cultured mrVSMCs.

Effect of ENaC Inhibition on Myogenic Vasoreactivity

To determine whether ENaC proteins are required for myogenic constriction, we evaluated myogenic constriction in isolated mouse interlobar arteries in the presence and absence of the specific ENaC inhibitors amiloride and benzamil. Under control conditions (Ca^{2+}-containing PSS) mouse interlobar arteries constricted in response to an increase in intraluminal pressure, whereas, when Ca^{2+} is removed from the bath, vessels distend passively to increases in intraluminal pressure (Fig. 4*A*). In control vessels, myogenic tone developed in a pressure-dependent manner and reached ~60% maximal myogenic tone at higher pressures. Amiloride (Fig. 4*B*) and benzamil (Fig. 4*C*) inhibited the development of myogenic tone by preventing active vasoconstriction. Passive inner diameter was not altered by amiloride or benzamil at any pressure point (data for 75 mmHg shown in Table 2).

Effect of ENaC Blockade on PE- and ACh-Induced Vasoreactivity

To determine whether amiloride and benzamil block vasoconstriction, per se, or specifically block stretch-mediated vasoconstriction, we evaluated vasoconstrictor and vasodilatory responses in isolated mouse interlobar arteries. As shown in Fig. 5, amiloride and benzamil did not inhibit PE-induced vasoconstriction (Fig. 5, *A* and *B*) or ACh-induced vasodilation (Fig. 5*C*). These results indicate amiloride and benzamil blockade of myogenic constriction is not due to an inability of the arteries to constrict.

Effect of ENaC Inhibition on Pressure and KCl-Induced Increases in Cytosolic Ca^{2+} and Na^{+}

We used fluorescence ion indicator dyes to determine whether ENaC blockade with amiloride or benzamil altered F_{Ca} and F_{Na} intensity associated with pressure-induced stretch. Fluorescence intensity did not change during pre- and post treatment with amiloride and benzamil, suggesting neither affect baseline fluorescence intensity (Table 2). Raising intraluminal pressure from 50 to 125 mmHg increased F_{Ca} and F_{Na} intensity, whereas amiloride (5 μM) and benzamil (1 μM) abolished pressure-induced increase in F_{Ca} and F_{Na} intensity (Fig. 6*A*). Summarized data are shown in Fig. 6, *B* and *C*. In contrast to pressure-induced changes, amiloride and benzamil did not inhibit KCl-induced increase in F_{Ca} intensity (Fig. 6*D*). Rather, benzamil treatment significantly increased KCl-induced F_{Ca} intensity compared with vehicle controls; the opposite of what we would predict if benzamil inhibited vasoconstriction by nonspecifically blocking Ca^{2+} mobilization. KCl did not increase F_{Na} intensity (Fig. 6*E*). Although voltage-gated Na^{+} channels have been reported in VSMCs isolated from conduit arteries (8, 27, 39, 41), they have not been identified in resistance vessels. Therefore, we do not expect high KCl (depolarizing stimulus) to increase F_{Na} intensity. Together, these results indicate amiloride and benzamil specifically block pressure-induced ion transients.

DISCUSSION

The aim of this study was to determine whether DEG/ENaC proteins are required for myogenic constriction. Results from our investigation indicate *1*) ENaC transcripts and proteins are expressed in renal VSMCs and *2*) DEG/ENaC activity is required for pressure-induced constriction and increases in cytosolic Ca^{2+} and Na^{+}. These data suggest DEG/ENaC proteins are required for myogenic constriction and support our hypothesis that DEG/ENaC proteins may act as mechanosensors that respond to changes in intraluminal pressure in vascular tissue.

Resistance vessels across many vascular beds respond to increases in blood pressure by constricting, a mechanism important for maintaining blood flow autoregulation. This response is independent of neural, metabolic, and hormonal vasoactive factors, but rather, initiated by conversion of a mechanical stimulus (pressure) into a cellular event (depolarization/constriction). Numerous molecules have been considered as potential mechanotransducers, including *1*) membrane-bound enzyme systems, *2*) activation of transporters and exchangers, and *3*) mechanosensitive ion channels (10). The latter has been the focus of several recent studies that suggested mechanosensitive cation-selective channels initiate pressure-induced contraction by depolarizing VSMCs past the threshold for activation of voltage-gated Ca^{2+} channels (9, 22, 29, 38, 42, 46).

DEG/ENaC proteins are expressed in a diverse range of species and cell types, where many are known to form cation-selective ion channels (33). Genetic evidence suggested that many DEG/ENaC family members are required for normal mechanosensation (7, 11, 21, 37, 44). Investigations regarding the role of DEG/ENaC proteins in mammals have focused

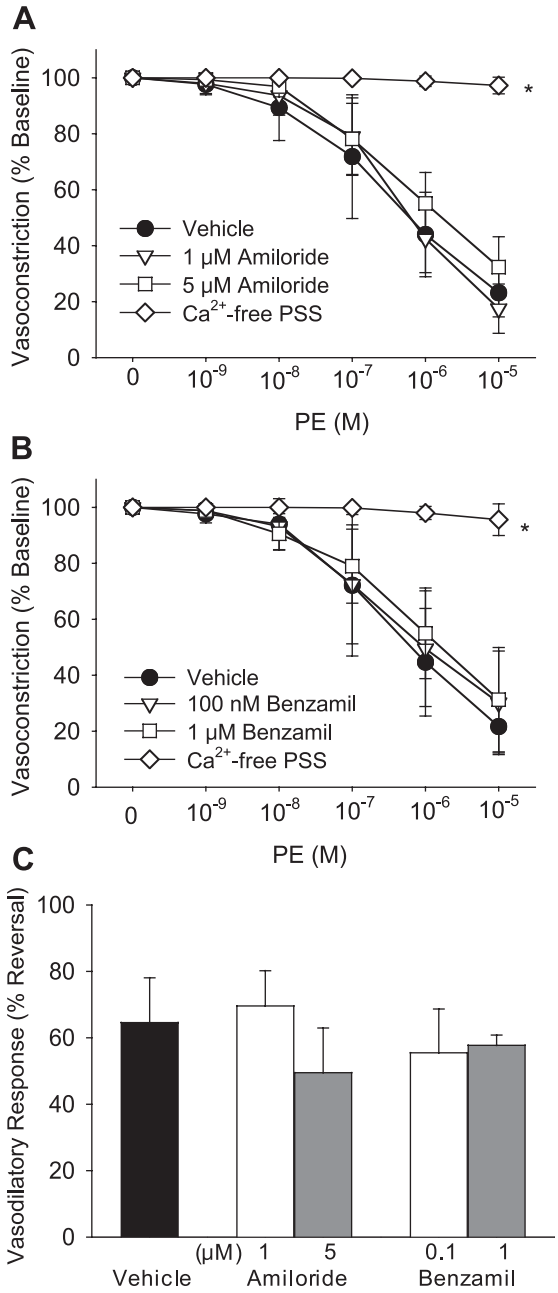

Fig. 5. Agonist-induced reactivity is unaltered by ENaC inhibition in isolated mouse interlobar arteries. Vasoconstriction (expressed as percent of baseline diameter) to the α_1-adgenergic receptor agonist phenylephrine (PE; 10^{-9}–10^{-5} M) in the presence of ENaC inhibitors is shown in *A* and *B*. Neither amiloride (*A*; 1 and 5 μM) nor benzamil (*B*; 0.1 and 1 μM) inhibit PE-induced vasoconstriction. *C*: vasodilatory responses to the endothelium-dependent vasodilator ACh (1 μM) in PE-constricted arteries are not inhibited by amiloride (1 and 5 μM) or benzamil (0.1 and 1 μM). Values are means ± SD (n = 5–6 in each group). *$P < 0.05$ vs. vehicle.

mainly on mechanotransduction in neuronal cells (13, 18, 34). Recently, our laboratory investigated the potential role of DEG/ENaC proteins as mechanosensors in VSMCs (14). In the present study, we aimed to determine whether ENaC proteins are involved in the renal myogenic response.

To begin to address the hypothesis that DEG/ENaC proteins form mechanosensitive ion channel complexes in VSMCs, we wanted to determine whether ENaC transcripts and proteins are expressed in mouse renal VSM. There are at least four known ENaC proteins in mammals, α, β, γ, and δ, although the latter has not been fully characterized. In cultured mrVSMCs, we detected α-, β-, and γENaC transcript and protein expression. However, in freshly dispersed mrVSMCs, we only detected β- and γ- but not αENaC protein. Although this is consistent with recent studies in our laboratory in rat cerebral VSMCs (14), most heterologous expression systems require coexpression of αENaC, with β- and γENaC, to generate constitutive ENaC activity (6). The lack of αENaC expression in fresh, but not cultured, VSMCs raises two very important questions. First, is αENaC required to form a channel? Second, why, and how, is αENaC expression activated in cultured VSMCs?

The lack of αENaC expression does not necessarily imply that β- and γENaC are unable to form a channel. Recent studies by Rossier and colleagues (4) demonstrated amiloride-sensitive current is present 6 days after βγrENaC expression in oocytes. These data suggest that β and γ can form a channel without α. In addition, β- and γENaC may require associated proteins, not present in the heterologous expression system, to mechanically gate the channel. We speculate that, in mechanosensitive tissue, βγENaC subunits form the pore of the channel and interact with integrins, extracellular matrix, and cytoskeletal proteins to form a larger mechanosensitive complex. This is supported by recent findings that accessory cytoskeletal proteins are required to mechanically gate a mechanosensitive channel formed by DEG proteins in *C. elegans* (37).

Unlike freshly dispersed cells, we readily detect αENaC protein in cultured mrVSMCs. This is not limited to mrVSMCs but also occurs in other cultured VSMC preparations (A10 and SV40LT cells; data not shown). The explanation for this finding is not known. However, we speculate αENaC expression in cultured VSMCs may represent an artifact of culturing, since expression of other ion channels and smooth muscle-specific proteins required for contraction are also altered after culture (43, 48). Alternatively, it is possible that the expression of αENaC in freshly dispersed mrVSMC is suppressed below our detectable range. Substances present in the culture media may stimulate αENaC expression or factors that normally suppress αENaC expression in vivo are absent in culture. These results raise the possibility that αENaC expression in VSMCs may be regulated by hormonal, paracrine, or autocrine substances, as other investigators have shown (3, 16, 19). It remains unclear whether αENaC is expressed in VSMCs in vivo.

To demonstrate a role for ENaC proteins in myogenic constriction in mouse renal interlobar arteries, we evaluated constrictor responses following ENaC inhibition with amiloride and benzamil. Similar to recent work by our laboratory and others (14, 24, 40), pressure-induced constriction is sensitive to amiloride, suggesting ENaC proteins may be required for myogenic constriction. The specificity of amiloride and benzamil blockade is critical to interpretation of the data. At concentrations >10–100 μM, amiloride and benzamil can block other transporters, exchangers, and channels that can indirectly alter contractility (31). Although amiloride and benzamil are considered to be specific for ENaC proteins at the concentrations used in this study, this has not been conclusively demonstrated. We show that 5 μM amiloride and 1 μM benzamil, concentrations that abolish myogenic constriction, do not inhibit vasoconstrictor responses to PE or vasodilatory

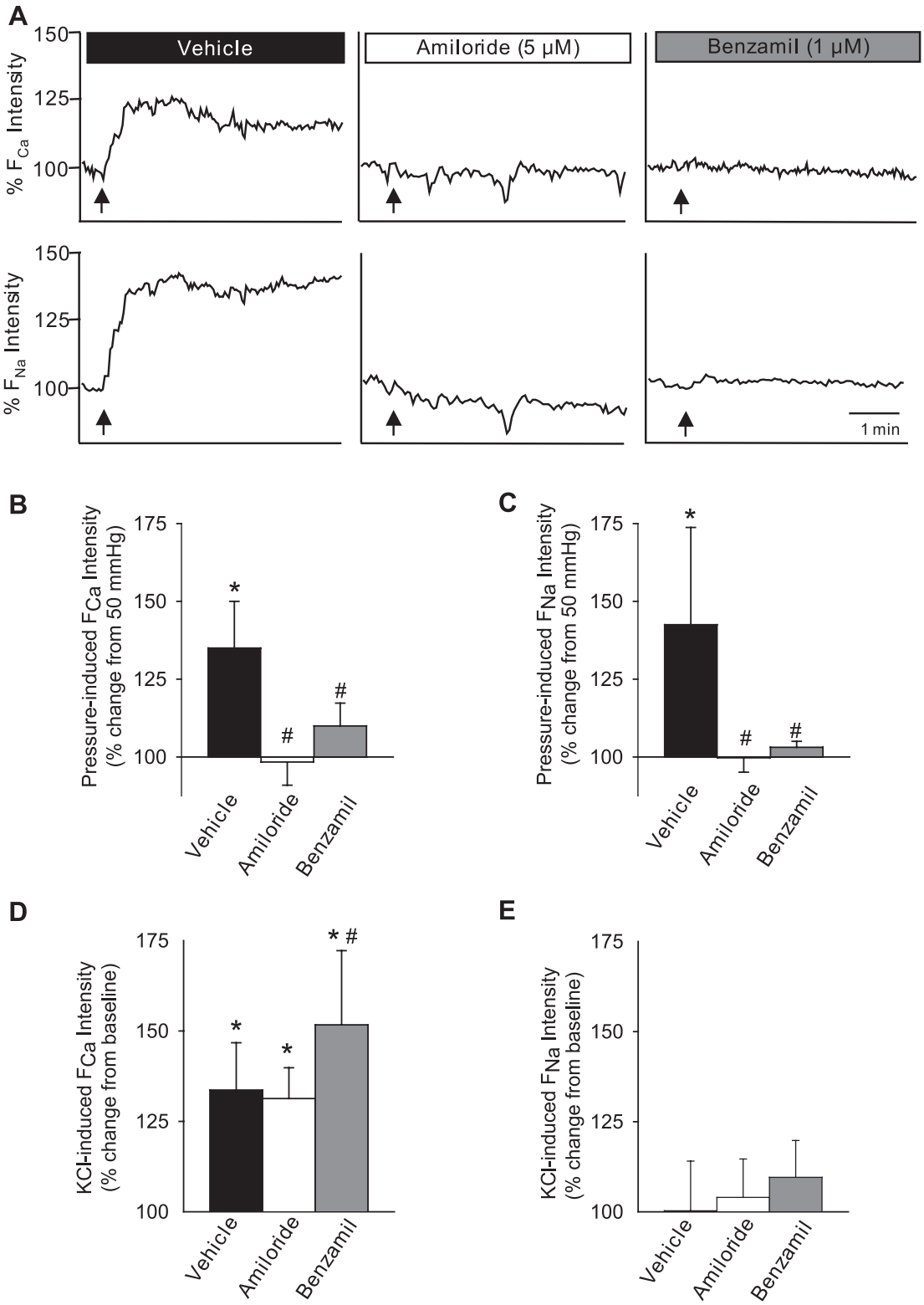

Fig. 6. ENaC inhibition blocks pressure-induced, but not KCl-induced, increases in Ca^{2+} and Na^{+} fluorescence (F_{Ca} and F_{Na}) intensity in isolated mouse interlobar arteries. *A*: representative traces demonstrate percent increase in F_{Ca} (*top left*) and F_{Na} (*bottom left*) intensity when intraluminal pressure is increased from 50 to 125 mmHg (indicated by arrow). The percent increases in F_{Ca} and F_{Na} intensity were abolished by amiloride (5 μM; *middle*) and benzamil (1 μM; *right*). Summarized data for percent change in F_{Ca} and F_{Na} are shown in *B* and *C*, respectively. KCl-induced increases in F_{Ca} intensity are not inhibited by ENaC blockade in isolated mouse interlobar arteries. *D*: Percent change in KCl (50 mM)-induced F_{Ca} intensity from baseline in the presence of vehicle, amiloride (5 μM), and benzamil (1 μM). *E*: KCl did not increase F_{Na} intensity. Amiloride and benzamil had no effect on F_{Na} intensity. Values are means ± SD ($n = 6$ in each group). *$P < 0.05$ vs. baseline. #$P < 0.05$ vs. vehicle.

responses to ACh. The data indicate that amiloride and benzamil block pressure-induced vasoconstriction, not vasoconstriction, per se. The ability of amiloride and benzamil to specifically block ENaC is also supported by our finding that amiloride and benzamil abolish pressure-induced increases in intracellular Ca^{2+} and Na^{+}, without decreasing KCl-induced Ca^{2+} increases. Although we cannot rule out pressure-induced intracellular release of Ca^{2+}, these studies suggest both Ca^{2+} and Na^{+} constitute the pressure-induced current that is dependent on ENaC proteins.

The role of ENaC proteins in the regulation of blood pressure has been described in kidney epithelial cells, where these channels play a rate-limiting role in Na^{+} and water transport. The present investigation demonstrates that ENaC proteins may also contribute to blood flow regulation, perhaps in their role as components of mechanosensitive ion channel complexes activated by stretch. The profound effect of ENaC blockade on myogenic constriction suggests this protein family may contribute significantly to renal autoregulation. Although our data are consistent with our hypothesis, they do not conclusively prove DEG/ENaC proteins are components of mechanosensitive ion channel complexes in VSM cells. Genetic models, such as ENaC knockout mice, are not feasible for investigation because the animals die shortly after birth due to defects in salt and water transport (1, 25, 35). Future experiments are needed to address the requirement of specific DEG/ENaC proteins for myogenic constriction using alternative tissue-targeted gene-silencing approaches.

ACKNOWLEDGMENTS

We thank Kim Parker and Angela Hoover for technical assistance and our laboratory colleagues Marise M. Furtado and Samira Grifoni for excellent discussion.

GRANTS

National Heart, Lung, and Blood Institute Grants HL-51971 and HL-071603 supported this work.

REFERENCES

1. **Barker PM, Nguyen MS, Gatzy JT, Grubb B, Norman H, Hummler E, Rossier B, Boucher RC, and Koller B.** Role of γ ENaC subunit in lung liquid clearance and electrolyte balance in newborn mice. Insights into perinatal adaptation and pseudohypoaldosteronism. *J Clin Invest* 102: 1634–1640, 1998.
2. **Benos DJ and Stanton BA.** Functional domains within the degenerin/epithelial sodium channel (Deg/ENaC) superfamily of ion channels. *J Physiol* 520: 631–644, 1999.
3. **Blazer-Yost BL, Liu X, and Helman SI.** Hormonal regulation of ENaCs: insulin and aldosterone. *Am J Physiol Cell Physiol* 274: C1373–C1379, 1998.
4. **Bonny O, Chraibi A, Loffing J, Jaeger NF, Grunder S, Horisberger JD, and Rossier BC.** Functional expression of a pseudohypoaldosteronism type I mutated epithelial Na^{+} channel lacking the pore-forming region of its α-subunit. *J Clin Invest* 104: 967–974, 1999.
5. **Brouard M, Casado M, Djelidi S, Barrandon Y, and Farman N.** Epithelial sodium channel in human epidermal keratinocytes: expression of its subunits and relation to sodium transport and differentiation. *J Cell Sci* 112: 3343–3352, 1999.
6. **Canessa C, Schild L, Buell G, Thorens B, Gautschi I, Horisberger J, and Rossier B.** Amiloride-sensitive epithelial Na^{+} channel is made of three homologous subunits. *Nature* 367: 463–467, 1994.
7. **Chalfie M and Wolinsky E.** The identification and suppression of inherited neurodegeneration in *Caenorhabditis elegans*. *Nature* 345: 410–416, 1990.
8. **Cox R, Zhou Z, and Tulenko T.** Voltage-gated sodium channels in human aortic smooth muscle cells. *J Vasc Res* 35: 310–317, 1998.
9. **Davis MJ, Donovitz JA, and Hood JD.** Stretch-activated single-channel and whole cell currents in vascular smooth muscle cells. *Am J Physiol Cell Physiol* 262: C1083–C1088, 1992.
10. **Davis MJ and Hill MA.** Signaling mechanisms underlying the vascular myogenic response. *Physiol Rev* 79: 387–423, 1999.
11. **Driscoll M and Chalfie M.** The mec-4 gene is a member of a family of *Caenorhabditis elegans* genes that can mutate to induce neuronal degeneration. *Nature* 349: 588–593, 1991.
12. **Drummond H, Abboud F, and Welsh M.** Localization of β and γ subunits of ENaC in sensory nerve endings in the rat foot pad. *Brain Res* 884: 1–12, 2000.
13. **Drummond H, Price M, Welsh M, and Abboud F.** A molecular component of the arterial baroreceptor mechanotransducer. *Neuron* 21: 1435–1441, 1998.
14. **Drummond HA, Gebremedhin D, and Harder DR.** Degenerin/epithelial Na^{+} channel proteins: components of a vascular mechanosensor. *Hypertension* 44: 643–648, 2004.
15. **Dubey R, Roy A, and Overbeck H.** Culture of renal arteriolar smooth muscle cells. Mitogenic responses to angiotensin II. *Circ Res* 71: 1143–1152, 1992.
16. **Gambling L, Dunford S, Wilson CA, McArdle HJ, and Baines DL.** Estrogen and progesterone regulate α, β, and γENaC subunit mRNA levels in female rat kidney. *Kidney Int* 65: 1774–1781, 2004.
17. **Garcia-Anoveros J and Corey DP.** The molecules of mechanosensation. *Annu Rev Neurosci* 20: 567–594, 1997.
18. **Garcia-Anoveros J, Samad TA, Zuvela-Jelaska L, Woolf CJ, and Corey DP.** Transport and localization of the DEG/ENaC ion channel BNaClα to peripheral mechanosensory terminals of dorsal root ganglia neurons. *J Neurosci* 21: 2678–2686, 2001.
19. **Garty H.** Regulation of the epithelial Na^{+} channel by aldosterone: Open questions and emerging answers. *Kidney Int* 57: 1270–1276, 2000.
20. **Garty H and Palmer LG.** Epithelial sodium channels: function, structure, and regulation. *Physiol Rev* 77: 359–396, 1997.
21. **Gu G, Caldwell GA, and Chalfie M.** Genetic interactions affecting touch sensitivity in *Caenorhabditis elegans*. *Proc Natl Acad Sci USA* 93: 6577–6582, 1996.
22. **Hajduczok G, Chapleau M, Ferlic R, Mao H, and Abboud F.** Gadolinium inhibits mechanoelectrical transduction in rabbit carotid baroreceptors. Implication of stretch-activated channels. *J Clin Invest* 94: 2392–2396, 1994.
23. **Harder D.** Pressure-dependent membrane depolarization in cat middle cerebral artery. *Circ Res* 55: 197–202, 1984.
24. **Henrion D, Laher I, Klaasen A, and Bevan JA.** Myogenic tone of rabbit facial vein and posterior cerebral artery is influenced by changes in extracellular sodium. *Am J Physiol Heart Circ Physiol* 266: H377–H383, 1994.
25. **Hummler E, Barker P, Gatzy J, Beermann F, Verdumo C, Schmidt A, Boucher R, and Rossier BC.** Early death due to defective neonatal lung liquid clearance in αENaC-deficient mice. *Nat Genet* 12: 325–328, 1996.
26. **Ismailov II, Awayda MS, Berdiev BK, Bubien JK, Lucas JE, Fuller CM, and Benos DJ.** Triple-barrel organization of ENaC, a cloned epithelial Na[IMAGE] channel. *J Biol Chem* 271: 807–816, 1996.
27. **James AF, Okada T, and Horie M.** A fast transient outward current in cultured cells from human pulmonary artery smooth muscle. *Am J Physiol Heart Circ Physiol* 268: H2358–H2365, 1995.
28. **Kellenberger S and Schild L.** Epithelial sodium channel/degenerin family of ion channels: a variety of functions for a shared structure. *Physiol Rev* 82: 735–767, 2002.
29. **Kirber M, Walsh JJ, and Singer J.** Stretch-activated ion channels in smooth muscle: a mechanism for the initiation of stretch-induced contraction. *Pflügers Arch* 412: 339–345, 1988.
30. **Kizer N, Guo XL, and Hruska K.** Reconstitution of stretch-activated cation channels by expression of the α-subunit of the epithelial sodium channel cloned from osteoblasts. *Proc Natl Acad Sci USA* 94: 1013–1018, 1997.
31. **Kleyman T and Cragoe EJ.** Amiloride and its analogs as tools in the study of ion transport. *J Membr Biol* 105: 1–21, 1988.
32. **Knot HJ and Nelson MT.** Regulation of membrane potential and diameter by voltage-dependent K^{+} channels in rabbit myogenic cerebral arteries. *Am J Physiol Heart Circ Physiol* 269: H348–H355, 1995.
33. **Mano I and Driscoll M.** DEG/ENaC channels: a touchy superfamily that watches its salt. *Bioessays* 21: 568–578, 1999.
34. **McCarter G, Reichling D, and Levine J.** Mechanical transduction by rat dorsal root ganglion neurons in vitro. *Neurosci Lett* 273: 179–182, 1999.

35. **McDonald FJ, Yang B, Hrstka RF, Drummond HA, Tarr DE, McCray PB Jr, Stokes JB, Welsh MJ and Williamson RA.** Disruption of the β subunit of the epithelial Na^+ channel in mice: hyperkalemia and neonatal death associated with a pseudohypoaldosteronism phenotype. *Proc Natl Acad Sci USA* 96: 1727–1731, 1999.
36. **Meininger GA and Davis MJ.** Cellular mechanisms involved in the vascular myogenic response. *Am J Physiol Heart Circ Physiol* 263: H647–H659, 1992.
37. **O'Hagan R, Chalfie M, and Goodman MB.** The MEC-4 DEG/ENaC channel of *Caenorhabditis elegans* touch receptor neurons transduces mechanical signals. *Nat Neurosci* 8: 43–50, 2005.
38. **Ohya Y, Adachi N, Nakamura Y, Setoguchi M, Abe I, and Fujishima M.** Stretch-activated channels in arterial smooth muscle of genetic hypertensive rats. *Hypertension* 31: 254–258, 1998.
39. **Okabe K, Kitamura K, and Kuriyama H.** The existence of a highly tetrodotoxin sensitive Na channel in freshly dispersed smooth muscle cells of the rabbit main pulmonary artery. *Pflügers Arch* 411: 423–428, 1988.
40. **Oyabe A, Masumoto N, Ueta K, and Nakayama K.** Amiloride-sensitive pressure-induced myogenic contraction in rat cerebral artery. *Fundam Clin Pharmacol* 14: 369–377, 2000.
41. **Quignard J, Ryckwaert F, Albat B, Nargeot J, and Richard S.** A novel tetrodotoxin-sensitive Na^+ current in cultured human coronary myocytes. *Circ Res* 80: 377–382, 1997.
42. **Takenaka T, Suzuki H, Okada H, Hayashi K, Kanno Y, and Saruta T.** Mechanosensitive cation channels mediate afferent arteriolar myogenic constriction in the isolated rat kidney. *J Physiol* 511: 245–253, 1998.
43. **Tang G and Wang R.** Differential expression of KV and KCa channels in vascular smooth muscle cells during 1-day culture. *Pflügers Arch* 442: 124–135, 2001.
44. **Tavernarakis N, Shreffler W, Wang S, and Driscoll M.** unc-8, a DEG/ENaC family member, encodes a subunit of a candidate mechanically gated channel that modulates *C. elegans* locomotion. *Neuron* 18: 107–119, 1997.
45. **Ugawa S, Minami Y, Guo W, Saishin Y, Takatsuji K, Yamamoto T, Tohyama M, and Shimada S.** Receptor that leaves a sour taste in the mouth. *Nature* 395: 555–556, 1998.
46. **Wellner M and Isenberg G.** Stretch-activated nonselective cation channels in urinary bladder myocytes: importance for pacemaker potentials and myogenic response. *EXS* 66: 93–99, 1993.
47. **Wu X and Davis MJ.** Characterization of stretch-activated cation current in coronary smooth muscle cells. *Am J Physiol Heart Circ Physiol* 280: H1751–H1761, 2001.
48. **Yuan XJ, Goldman WF, Tod ML, Rubin LJ, and Blaustein MP.** Ionic currents in rat pulmonary and mesenteric arterial myocytes in primary culture and subculture. *Am J Physiol Lung Cell Mol Physiol* 264: L107–L115, 1993.